JOC The Journal of Organic Chemistry

Article

Substituent and Solvent Effects on the β-Heterolysis Reaction of β-Hydroxy Arylethyl Radicals

Frances L. Cozens, Sandy F. Lancelot, and Norman P. Schepp

J. Org. Chem., **2007**, 72 (26), 10022-10028 • DOI: 10.1021/jo701874f

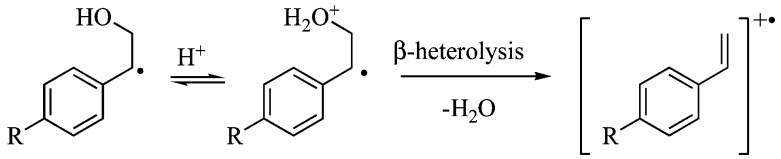

R = Cl, H, F, CH_3, and OCH_3

More About This Article

Additional resources and features associated with this article are available within the HTML version:

- Supporting Information
- Links to the 1 articles that cite this article, as of the time of this article download
- Access to high resolution figures
- Links to articles and content related to this article
- Copyright permission to reproduce figures and/or text from this article

View the Full Text HTML

The Journal of Organic Chemistry is published by the American Chemical Society.
1155 Sixteenth Street N.W., Washington, DC 20036

JOC Article

Substituent and Solvent Effects on the β-Heterolysis Reaction of β-Hydroxy Arylethyl Radicals

Frances L. Cozens,* Sandy F. Lancelot, and Norman P. Schepp*

Department of Chemistry, Dalhousie University, Halifax, Nova Scotia, Canada, B3H 4J3

fcozens@dal.ca

Received August 27, 2007

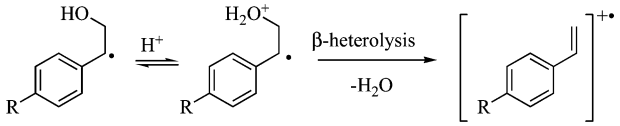

R = Cl, H, F, CH_3, and OCH_3

Time-resolved conversion of a series of β-hydroxy arylethyl radicals with electron-donating and -withdrawing aromatic substituents to their corresponding styrene radical cation via heterolytic loss of the β-hydroxy leaving group was examined with nanosecond laser flash photolysis. In all cases, the reaction was catalyzed by added perchloric acid. Radicals **2a**−**d** reacted via a pre-equilibrium protonation mechanism in acidic 1,1,1,3,3,3-hexafluoroisopropanol (HFIP), and measuring rate constants for radical cation formation as a function of acid content allowed for the determination of absolute rate constants ranging from 3.6×10^6 to 3.8×10^7 s^{-1} for the loss of water from the protonated β-hydroxy arylethyl radicals **2a**−**d**, as well as the acidity constants, $pK_a \approx 1.5$ (in HFIP), for the protonated radicals. The 4-methoxy-substituted β-hydroxy arylethyl radical **2e** reacted by rate determining protonation in HFIP with a second-order rate constant of $k_{H^+} = 7.8 \times 10^8$ M^{-1} s^{-1}. However, in acetonitrile, 2,2,2-trifluoroethanol, and mixtures of these two solvents, **2e** reacted by pre-equilibrium protonation, allowing for solvent effects on the rate constant for loss of water from the protonated radical **2e** to be determined. With use of these data, substituent electronic effects on the kinetics of the β-heterolysis reaction are discussed. Differences in the effect of solvent on the rate constant for loss of water from the protonated β-hydroxy arylethyl radicals and other β-substituted arylethyl radicals are also discussed.

Introduction

Over the past two decades, it has become increasingly evident that organic free radicals can play key roles in a wide variety of different biological events.[1−5] One type of biologically derived radicals that have attracted considerable attention are radicals with a leaving group attached to the carbon adjacent (β) to the radical center. More specifically, the ionization of these radicals through heterolytic loss of the leaving group has been associated with reactions catalyzed by enzymes such as diol dehydrase,[1,6] ethanolamine deaminase,[1,7,8] and ribonucleotide reductase.[5,9,10]

In recent years, there has been considerable effort directed toward understanding the effect of radical structure and solvent on the dynamics and mechanisms of the bond heterolysis reaction of these kinds of radicals.[11−24] Special attention has been given to α-hydroxy and α-methoxy ketyl radicals, eq 1,

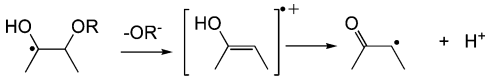

R = H, CH_3 (1)

as these radicals are models for some of those generated enzymatically.[25−27] Studying the dynamics of the heterolysis

(1) Frey, P. A. *Chem. Rev.* **1990**, *90*, 1343−1357.
(2) Fontecave, M. *CMLS Cell. Mol. Life Sci.* **1998**, *54*, 684−695.
(3) Stubbe, J. *Biochemistry* **1988**, *27*, 3893−3900.
(4) Stubbe, J. *Annu. Rev. Biochem.* **1989**, *58*, 257−285.
(5) Stubbe, J.; van der Donk, W. A. *Chem. Rev.* **1998**, *98*, 705−762.
(6) Smith, D. M.; Golding, B. T.; Radom, L. *J. Am. Chem. Soc.* **2001**, *123*, 1664−1675.
(7) Warncke, K.; Schmidt, J. C.; Ke, S.-C. *J. Am. Chem. Soc.* **1999**, *121*, 10522−10528.
(8) Warncke, S.-C. K. a. K. *J. Am. Chem. Soc.* **1999**, *121*, 9922−9927.
(9) Siegbahn, P. E. M. *J. Am. Chem. Soc.* **1998**, *120*, 8417−8429.
(10) Lenz, R.; Giese, B. *J. Am. Chem. Soc.* **1997**, *119*, 2784−2794.

10.1021/jo701874f CCC: $37.00
Published on Web 11/16/2007

SCHEME 1

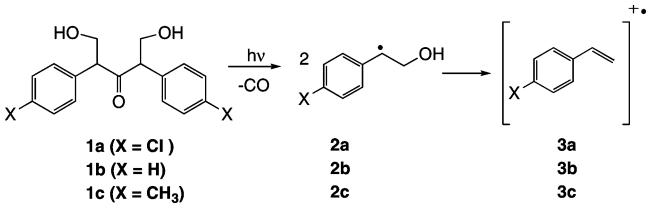

reaction[15] of these β-OR ketyl radicals is sometimes complicated by difficulties associated with time-resolved detection of the transient products. In particular, enol radical cations, if present as intermediates, are highly acidic and typically short-lived,[28−30] and α-acyl radicals[28,31] often are not easily observed or distinguished from the β-OR ketyl radical with UV spectroscopy, a convenient spectroscopic method for monitoring fast reactions in solution. Thus, in a manner similar to our earlier studies into the effect of variables such as ionizing ability of solvent and leaving group ability on the β-heterolysis of β-substituted phenethyl radicals,[11,12] we have now examined the time-resolved formation of styrene radical cations **3** from β-hydroxy arylethyl radicals **2** generated by photohomolysis of substituted dibenzyl ketones **1a**−**c**, Scheme 1, or benzyl methyl ketones **1d**,**e**, Scheme 2. Since these β-OH radicals are not ketyl radicals, the radical cations generated upon loss of the β-OH group are readily observed with UV−vis spectroscopy, and the dynamics of the heterolysis reaction could easily be studied as a function of substituent on the aromatic ring, solvent polarity, and acid content with laser flash photolysis.

SCHEME 2

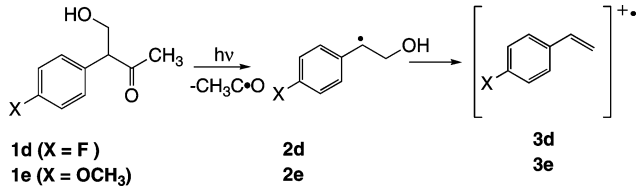

Results

Generation of β-Hydroxy Arylethyl Radicals. As shown in Figure 1a, 266 nm laser flash photolysis of the 4-Cl-substituted precursor **1a** in nitrogen-saturated acetonitrile (AcN) at 22 °C generated a transient with an absorption maximum near 270 nm. In nitrogen-purged AcN, this transient decayed in a second-order manner and was relatively long-lived, Figure 1a (inset). The transient was rapidly quenched under oxygenated conditions, Figure 1a. The location of the absorption maximum is reminiscent of benzyl radicals that absorb in the low-UV region, with the 4-chlorobenzyl radical possessing an absorption maximum near 280 nm.[32,33] It is also well-known that benzyl radicals are sensitive to radical scavengers and react rapidly with molecular oxygen.[32] Thus, we assign the transient at 270 nm to the β-hydroxy-(4-chlorophenyl)ethyl radical **2a** (X = Cl) produced by photoinduced α-cleavage[34−38] and decarbonylation[39−42] as shown in eq 2.

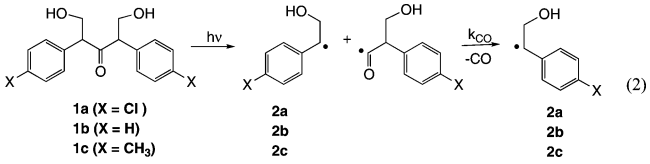

(2)

Laser flash photolysis of compounds **1b** and **1c** in nitrogen-saturated AcN resulted in the formation of transient species with similar spectral features, Figures 1b and 1c, to those described above. The transient absorption spectra show maxima near 280 nm, with additional sharp bands near 315 nm, that were completely quenched when laser irradiation was carried out in oxygenated AcN. The transients responsible for these absorption bands possess spectral profiles that closely resemble those reported for the benzyl radical and the 4-methylbenzyl radical, respectively.[32,33,43] The absorption maxima detected in these

(11) Cozens, F. L.; O'Neill, M.; Bogdanova, R.; Schepp, N. *J. Am. Chem. Soc.* **1997**, *119*, 10652−10659.
(12) Lancelot, S. F.; Cozens, F. L.; Schepp, N. P. *Org. Biomol. Chem.* **2003**, *1*, 1972−1979.
(13) Bales, B. C.; Horner, J. H.; Huang, X.; Newcomb, M.; Crich, D.; Greenberg, M. M. *J. Am. Chem. Soc.* **2001**, *123*, 3623−3629.
(14) Beckwith, A. L. J.; Crich, D.; Duggan, P. J.; Yao, Q. *Chem. Rev.* **1997**, *97*, 3273−3312.
(15) Crich, D.; Brebion, F.; Suk, D. H. In *Radicals in Synthesis I*: *Methods and Mechanisms*; Springer: New York, 2006; Vol. 263, pp 1−38.
(16) Horner, J. H.; Taxil, E.; Newcomb, M. *J. Am. Chem. Soc.* **2002**, *124*, 5402−5410.
(17) Horner, J. H.; Bagnol, L.; Newcomb, M. *J. Am. Chem. Soc* **2004**, *126*, 14979−14987.
(18) Horner, J. H.; Lal, M.; Newcomb, M. *Org. Lett.* **2006**, *8*, 5497−5500.
(19) Miranda, N.; Xu, L. B.; Newcomb, M. *Org. Lett.* **2004**, *6*, 4511−4514.
(20) Newcomb, M.; Horner, J. H.; Whitted, P. O.; Crich, D.; Huang, X.; Yao, Q.; Zipse, H. *J. Am. Chem. Soc.* **1999**, *121*, 10685−10694.
(21) Newcomb, M.; Miranda, N.; Huang, X.; Crich, D. *J. Am. Chem. Soc.* **2000**, *122*, 6128−6129.
(22) Newcomb, M.; Miranda, N.; Sannigrahi, M.; Huang, X. H.; Crich, D. *J. Am. Chem. Soc* **2001**, *123*, 6445−6446.
(23) Taxil, E.; Bagnol, L.; Horner, J. H.; Newcomb, M. *Org. Lett.* **2003**, *5*, 827−830.
(24) Whitted, P. O.; Horner, J. H.; Newcomb, M.; Huang, X.; Crich, D. *Org. Lett.* **1999**, *1*, 153−156.
(25) Newcomb, M.; Miranda, N. *J. Org. Chem.* **2004**, *69*, 6515−6520.
(26) Steenken, S.; Davies, M. J.; Gilbert, B. C. *J. Chem. Soc., Perkin Trans. 2* **1986**, 1003−1010.
(27) Xu, L. B.; Newcomb, M. *J. Org. Chem.* **2005**, *70*, 9296−9303.
(28) Schepp, N. P. *J. Org. Chem.* **2004**, *69*, 4931−4935.
(29) Schmittel, M.; Gescheidt, G.; Rock, M. *Angew. Chem., Int. Ed. Engl.* **1994**, *33*, 1961−1963.
(30) Schmittel, M. In *Electron Transfer I*; Springer-Verlag: New York, 1994; Vol. 169, pp 183−230.
(31) Bejan, E. V.; Font-Sanchis, E.; Scaiano, J. C. *Org. Lett.* **2001**, *3*, 4059−4062.
(32) Tokumura, K.; Ozaki, T.; Nosaka, H.; Saigusa, Y.; Itoh, M. *J. Am. Chem. Soc.* **1991**, *113*, 4974−4980.
(33) Claridge, R. F. C.; Fischer, H. *J. Phys. Chem.* **1983**, *87*, 1960−1967.
(34) Engel, P. S. *J. Am. Chem. Soc.* **1970**, *92*, 6074−6076.
(35) Robbins, W. K.; Eastman, R. H. *J. Am. Chem. Soc.* **1970**, *92*, 6076−6077.
(36) Robbins, W. K.; Eastman, R. H. *J. Am. Chem. Soc.* **1970**, *92*, 6077−6079.
(37) Gould, I. R.; Baretz, B. H.; Turro, N. J. *J. Phys. Chem.* **1987**, *91*, 925−929.
(38) Arbour, C.; Atkinson, G. H. *Chem. Phys. Lett.* **1989**, *159*, 520−525.
(39) Zhang, X.; Nau, W. M. *J. Phys. Org. Chem.* **2000**, *13*, 634−639.
(40) Tsentalovich, Y. P.; Fischer, H. *J. Chem. Soc., Perkin Trans. 2* **1994**, 729−733.
(41) Turro, N. J.; Gould, I. R.; Baretz, B. H. *J. Phys. Chem.* **1983**, *87*, 531−532.
(42) Lunazzi, L.; Ingold, K. U.; Scaiano, J. C. *J. Phys. Chem.* **1983**, *87*, 529−530.
(43) Chatgilialoglu, C. In *Handbook of Organic Photochemistry*; Scaiano, J. C., Ed.; CRC Press: Boca Raton, FL, 1989; Vol. 2, pp 3−11.

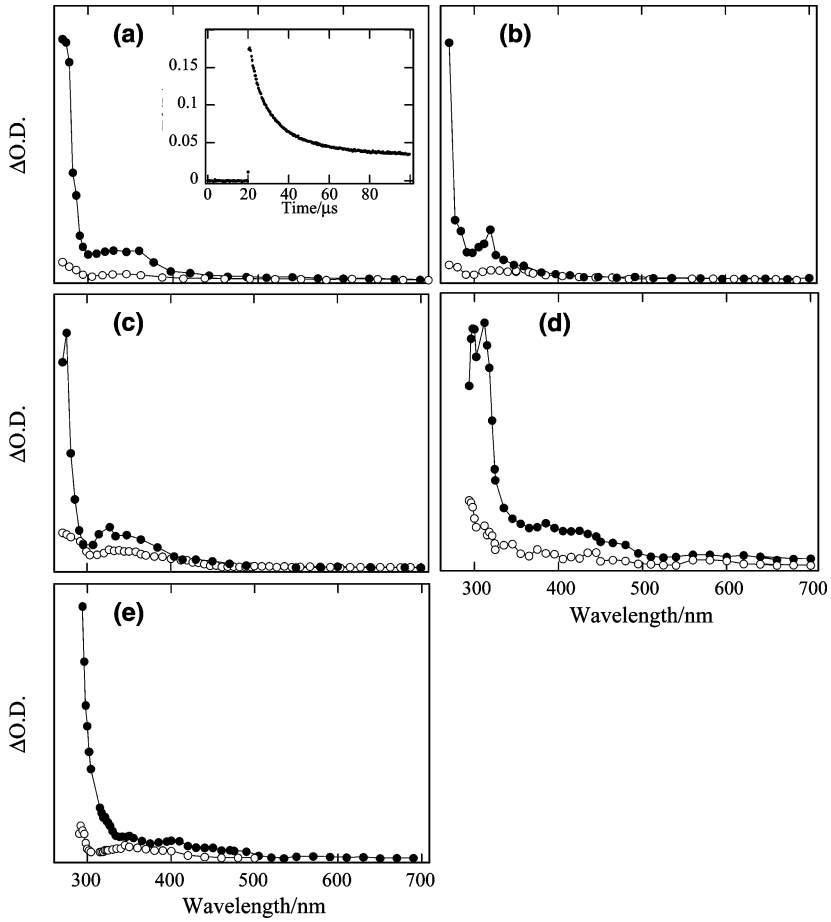

FIGURE 1. Transient absorption spectra obtained 0.60 μs after 266 nm laser irradiation of (a) 2,4-bis(4-chlorophenyl)-1,5-dihydroxy-3-pentanone **1a**, (b) 2,4-diphenyl-1,5-dihydroxy-3-pentanone **1b**, (c) 2,4-bis(4-methylphenyl)-1,5-dihydroxy-3-pentanone **1c**, (d) 3-(4-fluorophenyl)-4-hydroxy-2-butanone **1d**, and (e) 3-(4-methoxyphenyl)-4-hydroxy-2-butanone **1e** in (●) nitrogen-saturated and (○) oxygen-saturated acetonitrile.

experiments are therefore attributed to the β-hydroxy arylethyl radicals **2b** and **2c** generated according to the mechanism shown in eq 2.

No time-resolved growth in absorption at 280−300 nm was observed after laser irradiation of precursors **1a**−**c**. Since the first 50−100 ns after the laser pulse was inaccessible due to strong, laser-induced luminescence from the sample, the absence of time-resolved growth indicates that the second benzylic radical formed by loss of carbon monoxide occurred with a rate constant greater than ca. 1×10^7 to 2×10^7 s^{-1}. The rate constant for decarbonylation of the α-methylbenzylacetyl radical in acetonitrile or other polar solvents has not been measured, but is rapid in isooctane where $k_{-CO} = 4.9 \times 10^7$ s^{-1}.[44] The rate constants for decarbonylation of other similar radicals, such as the benzylacetyl radical, are 2−3 times slower in acetonitrile and hydroxylic solvents such as acetic acid and methanol than in hexane.[39,45] Assuming the same rate reduction would be observed for the α-methylbenzylacetyl radical in polar solvents, the rate constant for decarbonylation would still be greater than 1.5×10^7 s^{-1} and would be too rapid to observe.

The benzyl methyl ketone precursors **1d** and **1e** gave similar results following 266 nm laser excitation, respectively, in nitrogen-saturated AcN. The transient absorption spectra, Figures 1d and 1e, reveal absorption bands near 300 nm that, in both cases, were quenched by the addition of oxygen to the solution. These transient signals closely match those reported for the similar 4-fluoro and 4-methoxybenzyl radicals[32,33] and are assigned to the corresponding radicals **2d** and **2e** generated by photoinduced α-cleavage,[46] eq 3.

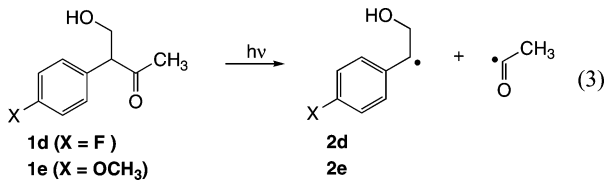

(3)

Laser Irradiation in Acidic AcN. Figure 2a shows the transient absorption spectra obtained upon laser irradiation of **1e** (X = CH_3O) in nitrogen-saturated AcN containing 4 mM perchloric acid. The initial spectrum obtained after the laser pulse contains the same absorption below 300 nm as observed in the spectrum obtained with nonacidic AcN (Figure 1e) and this absorption can be attributed to the β-hydroxy radical **2e**. However, unlike the situation in nonacidic AcN where radical **2e** decayed slowly, radical **2e** in acidic AcN decayed much more rapidly and as it decayed gave rise to two new absorption bands,

(44) Gould, I. R.; Baretz, B. H.; Turro, N. J. *J. Phys. Chem* **1987**, *91*, 925−929.

(45) Kurnysheva, O. A.; Gritsan, N. P.; Tsentalovich, Y. P. *Phys. Chem. Chem. Phys.* **2001**, *3*, 3677−3682.

(46) Ogata, Y.; Takagi, K.; Izawa, Y. *Tetrahedron* **1968**, *24*, 1617−1621.

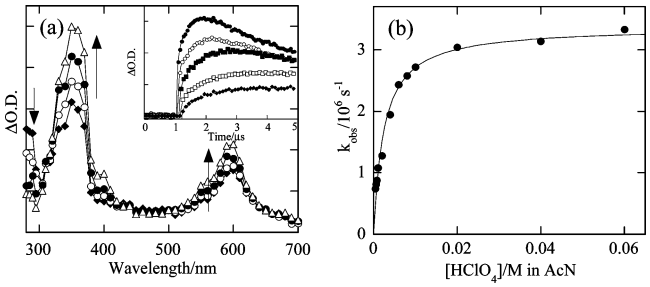

FIGURE 2. (a) Transient absorption spectra obtained (♦) 0.27, (○) 0.39, (●) 0.54, and (Δ) 1.2 μs after 266 nm laser irradiation of 3-(4-methoxyphenyl)-4-hydroxy-2-butanone **1e** in nitrogen-saturated acetonitrile containing 4 mM perchloric acid. The inset shows kinetic traces at 590 nm obtained in nitrogen-saturated acetonitrile containing (♦) 0.6, (□) 0.8, (■) 2, (○) 4, and (●) 10 mM perchloric acid. (b) Observed rate constants for the growth of the 4-methoxystyrene radical cation **3e** measured at 590 nm following 266 nm laser irradiation of **1e** in nitrogen-saturated acetonitrile plotted as a function of perchloric acid concentration.

one at 350 nm and the other at 600 nm. These two absorption bands grew in intensity in a first-order manner with identical rate constants of $k_{obs} = 1.9 \times 10^6$ s^{-1}, indicating that both bands correspond to a single transient species. Moreover, these growth rate constants matched closely the decay of the radical at 290 nm, $k_{obs} = 1.7 \times 10^6$ s^{-1}, which shows that the transient at 350 and 600 nm was a product from the reaction of the β-hydroxy radical.

The absorption spectrum of the new transient is identical with the absorption spectrum of the 4-methoxystyrene radical cation in acetonitrile,[47] which allows the new transient to be identified as radical cation **3e**. Furthermore, because the generation of radical cation **3e** required the presence of an acid, and because the radical cation growth dynamics matched the decay dynamics for the initially generated radical **2e**, it is reasonable to suggest that the mechanism for the formation of the radical cation involves initial protonation of the hydroxy group of the β-hydroxy radical to give the protonated radical, followed by elimination of water, eq 4 (X = OCH_3).[48]

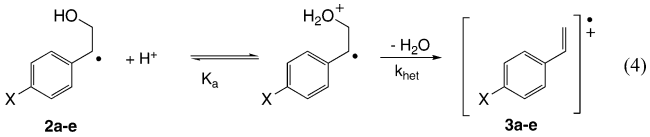

(4)

As illustrated in Figure 2a (inset), the growth of the radical cation **3e** became more rapid as the concentration of perchloric acid increased from 0.6 to 10 mM. Figure 2b shows that the rate constants for the growth of the radical cation increased in a linear manner with respect to acid concentration up to ca. 8 mM $HClO_4$, but then began to curve and eventually leveled off at a rate constant near $k_{obs} = 3 \times 10^6$ s^{-1}. This behavior is consistent with eq 5, which was derived from the mechanism in eq 4 by using the assumption that formation of the neutral radical/protonated radical equilibrium is complete prior to elimination of water, and that elimination of water from the protonated β-hydroxy radical is rate limiting.

$$k_{obs} = \frac{k_{het}[H^+]}{[H^+] + K_a} \quad (5)$$

According to this equation, when $[H^+]$ is less than the acidity constant, K_a, for the protonated radical, eq 5 reduces to $k_{obs} = k_{het}[H^+]/K_a$ and the observed rate constant for heterolysis increases in a linear manner with respect to acid concentration. At higher concentrations, $[H^+] > K_a$, eq 5 reduces to $k_{obs} = k_{het}$, and the rate constants become independent of acid concentration. The data in Figure 2b fit well to eq 5, and linear least-squares fitting of the data gave values of $k_{het} = 3.4 \times 10^6$ s^{-1} and $K_a = 2.4 \times 10^{-3}$ M, or p$K_a = 2.6$.

Radical cations **3a** to **3d** have previously been observed upon photoionization of their neutral styrene form in the weakly nucleophilic, ionizing solvent 2,2,2-trifluoroethanol (TFE), but were not observed in acetonitrile where they presumably are too reactive to be detected by nanosecond laser flash photolysis.[47] Thus, even if radicals **2a** to **2d** underwent rapid β-heterolysis in acidic acetonitrile, the radicals cation **3a** to **3d** would not be detectable, and reliable information about the rate constants for heterolysis could not be easily obtained. Indeed, laser irradiation of **1c** (X = CH_3) in acidic acetonitrile failed to yield detectable amounts of the radical cation **3c**, even in the presence of 60 mM $HClO_4$. As a result, laser photolysis experiments were carried out with acidic 1,1,1,3,3,3-hexafluoroisopropanol (HFIP), which is even more weakly nucleophilic and ionizing than TFE, and should be a solvent in which all of the radical cations **3a** to **3e** are sufficiently long-lived to be observed with nanosecond laser flash photolysis.

Laser Irradiation in Acidic HFIP. The transient absorption spectra in Figure 3 were obtained following 266 nm laser flash photolysis of **1a** to **1e** in nitrogen-saturated acidic ($HClO_4$) HFIP. In each case, a time-resolved growth was observed for two absorption bands, one at low wavelengths near 350 nm and the second at longer wavelengths near 600 nm. These absorption bands correspond nicely with the known absorption bands[47,49] of the radical cations **3a** to **3e**, which leads to the conclusion that the observed growths in absorption in Figure 3 were due to the formation of the corresponding radical cations. Figure 3 also shows the presence of absorption bands at lower wavelengths near 280−300 nm that correspond nicely with the spectra of radicals **2a**−**e** described earlier. In acidic HFIP, the rate constant for the decay of these radicals matched well the rate constant for the growth of the radical cations, indicating that the radical cations were products from the reaction of the radicals. Furthermore, as shown in Figure 4, the rate constants for the growth of the radical cations **3a**−**d** were affected by acid concentration in the same manner as described above for the growth of **3e** in acidic acetonitrile. Thus, the mechanism for the formation of the radical cations in acidic HFIP is the same as shown in eq 4, and involves initial protonation of the β-hydroxy radical, followed by rate determining β-heterolysis and loss of water to give the radical cation. The curves in Figure 4 fit well to eq 5, giving the rate constants, k_{het}, and acidity constants, K_a, summarized in Table 1 (first 4 entries).

The acid-catalyzed conversion of radical **2e** to radical cation **3e** in HFIP could only be monitored in acid concentrations up

(47) Johnston, L. J.; Schepp, N. P. *J. Am. Chem. Soc.* **1993**, *115*, 6564−6571.

(48) It is possible that the precursor is partially protonated in acidic HFIP. If so, the radical/protonated radical equilibrium state in eq 4 might be accessed from both the neutral radical and the protonated radical sides of the equilibrium. This situation does not affect the analysis for the elimination of water from the radical, since the radical/protonated radical pre-equilibrium state will still be established prior to the elimination step.

(49) Schepp, N. P.; Johnston, L. J. *J. Am. Chem. Soc.* **1994**, *116*, 6895−6903.

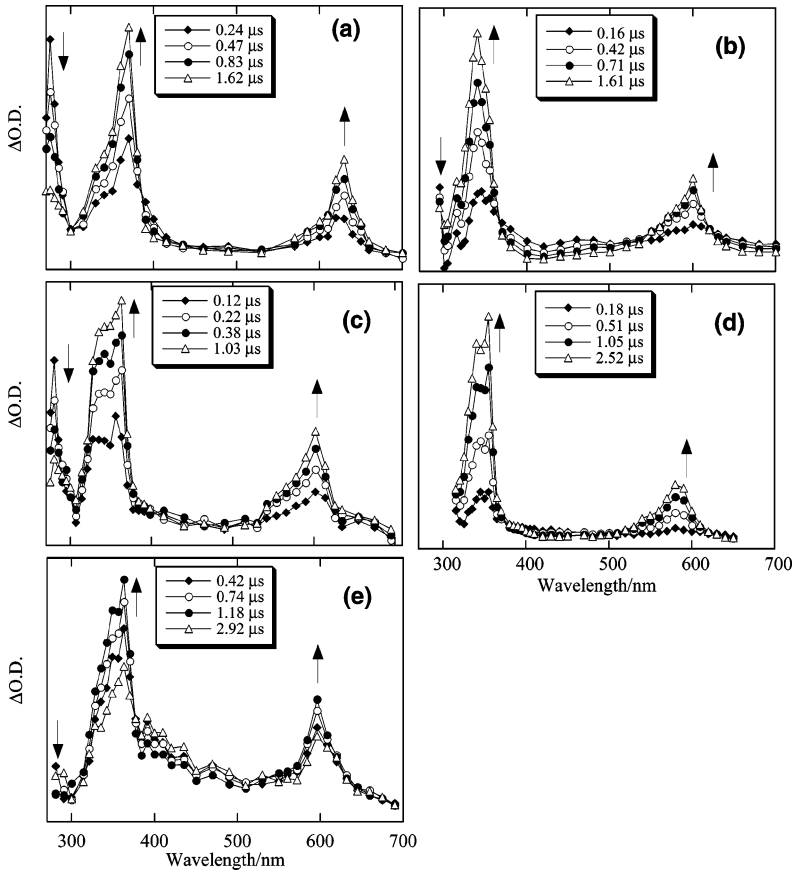

FIGURE 3. Transient absorption spectra obtained after 266 nm laser irradiation of (a) 2,4-bis(4-chlorophenyl)-1,5-dihydroxy-3-pentanone **1a**, $[HClO_4] = 0.021$ M, (b) 2,4-diphenyl-1,5-dihydroxy-3-pentanone **1b**, $[HClO_4] = 0.0078$ M, (c) 2,4-bis(4-methylphenyl)-1,5-dihydroxy-3-pentanone **1c**, $[HClO_4] = 0.010$ M, (d) 3-(4-fluorophenyl)-4-hydroxy-2-butanone **1d**, $[HClO_4] = 0.0049$ M, and (e) 3-(4-methoxyphenyl)-4-hydroxy-2-butanone **1e**, $[HClO_4] = 0.0028$ M, in nitrogen-saturated acidic HFIP. Boxes in each spectra indicate the time after the laser pulse that each spectrum was obtained.

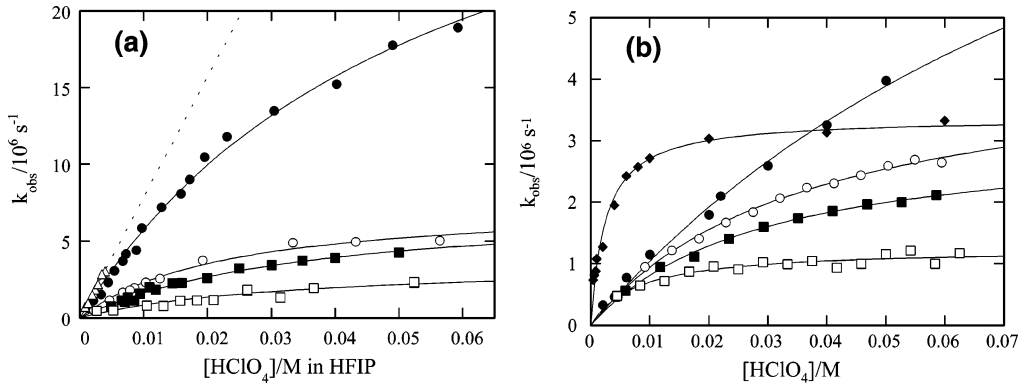

FIGURE 4. (a) Relationships between the observed rate constants for the elimination of water from β-OH radicals (□) **2a** (X = 4-Cl), (■) **2d** (X = 4-F), (○) **2b** (X = H), (●) **2c** (X = CH_3), and (Δ) **2e** (X = 4-CH_3O) and perchloric acid concentrations ranging from 1 to 60 mM in nitrogen-saturated HFIP. (b) Relationship between observed rate constants for the elimination of water from β-OH radical **2e** (X = 4-CH_3O) and perchloric acid concentration in (●) TFE, (○) 25% AcN:75% TFE, (■) 50% AcN:50% TFE, (□) 75% AcN:25% TFE, and (♦) AcN.

to 4 mM, which is about 10-fold lower than the acid concentrations used for the reaction of the other radicals. At higher acid concentrations, absorption due to radical **2e** and radical cation **3e** became weak and rate constants for the growth of the radical cation could no longer be measured. Since no curvature in the relationship between rate constants for the heterolysis reaction and acid concentrations was observed, these data were fit to a simple linear expression, $k_{obs} = k_{H^+}[H^+]$, giving $k_{H^+} = 78.1 \times 10^8$ M^{-1} s^{-1}.

Laser Irradiation in Acidic TFE and TFE/AcN Mixtures. Laser irradiation of **1e** in TFE and TFE/AcN mixtures with $HClO_4$ also led to conversion of the initially formed β-hydroxy radical **2e** to the corresponding 4-methoxystyrene radical cation **3e** by β-heterolysis. The rate constants for the growth of the radical cation as a function of acid concentration in these solvents are shown in Figure 4b, together with the data described earlier in acidic AcN. The data obtained in AcN and in the TFE/AcN mixtures were all clearly curved, and were treated by using

TABLE 1. Rate and Equilibrium Constants for the Elimination of Water from β-OH Radicals 2a−e in Acidic HFIP, AcN, TFE, and TFE/AcN (% volume) Mixtures (22 ± 1 °C)

radical	solvent	k_{het}/s^{-1}	K_a/M	pK_a
2a	HFIP	$(3.6 \pm 0.1) \times 10^6$	0.033 ± 0.004	1.5 ± 0.1
2b	HFIP	$(7.6 \pm 0.5) \times 10^6$	0.023 ± 0.003	1.6 ± 0.1
2c	HFIP	$(38 \pm 2) \times 10^6$	0.056 ± 0.005	1.3 ± 0.1
2d	HFIP	$(7.5 \pm 0.5) \times 10^6$	0.036 ± 0.003	1.4 ± 0.1
2e	AcN	$(3.4 \pm 0.1) \times 10^6$	0.0021 ± 0.0002	2.6 ± 0.1
2e	25% TFE/75% AcN	$(1.2 \pm 0.1) \times 10^6$	0.0078 ± 0.0014	2.1 ± 0.1
2e	50% TFE/50% AcN	$(3.1 \pm 0.1) \times 10^6$	0.029 ± 0.002	1.5 ± 0.1
2e	75% TFE/25% AcN	$(4.4 \pm 0.1) \times 10^6$	0.037 ± 0.002	1.4 ± 0.1
2e	TFE	$(12 \pm 2) \times 10^6$	0.11 ± 0.003	0.96 ± 0.1

eq 5 to give values for k_{het} and K_a in Table 1. The data obtained in neat TFE displayed considerably less curvature. However, since slight curvature was still evident, these data were also fit to eq 5 to give the k_{het} and pK_a values in Table 1.

Discussion

Earlier pulse radiolysis studies[26,50] led to the conclusion that β-OH ketyl radicals undergo acid-catalyzed loss of OH in aqueous solution according to a mechanism that involves a pre-equilibrium protonation of the leaving group, followed by loss of water to give a radical cation that then deprotonates to give an α-acyl radical, eq 6. The analogous mechanism in eq 4 is

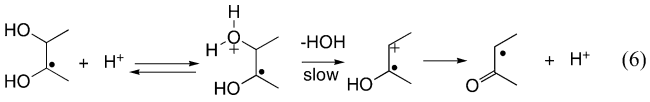

(6)

consistent with the curved plots obtained for the β-heterolysis of the OH group from radicals **2a** to **2d** to give radical cations **3a** to **3d**, except that radical cations **3a** to **3d** have no acidic protons and therefore have a sufficiently long lifetime to be readily detected by nanosecond laser flash photolysis.

Treatment of the rate constant data obtained at different acid concentrations by using eq 5 gave two parameters that define the overall dynamics for the reaction. One of these parameters is the acidity constant for the distonic radical cations generated by protonation of the radical, and the other parameter is the rate constant for elimination of water from the protonated radical, k_{het}, to give the styrene radical cation. As shown in Table 1, the rate constants for this heterolysis step depend on the nature of the aromatic substituent. For example, k_{het} for loss of water from the protonated 4-Cl radical **2a**, $k_{het} = 3.6 \times 10^6\ s^{-1}$, is significantly smaller than the rate constants for the same reaction of the 4-F **2d** and 4-H **2b** radicals, $k_{het} = 7.5 \times 10^6\ s^{-1}$ and $7.6 \times 10^6\ s^{-1}$, respectively. A much larger 5-fold increase in k_{het} then takes place upon going to the 4-CH_3 radical **2c**, $3.8 \times 10^7\ s^{-1}$.

The effect of substituents is quantitatively described in the Hammett plot in Figure 5. The negative slope of $\rho^+ = -2.60$ reflects the observations that the rate constant for the heterolysis process is increased by electron-donating substituents, and suggests a positive charge buildup as the reaction progresses from the starting material to the product. Of course, the protonated, or distonic radical cation, form of radicals **2a−d** already bears a full positive charge and no charge is being created on the substrate as the reaction progresses from the distonic radical cation to the transition state. However, the positive charge in the starting structure is localized on the oxygen atom and is not in direct resonance with the aromatic substituent. Thus, as the reaction proceeds and the carbon−oxygen atom bond breaks, a progressive redistribution of charge takes place whereby the original positive charge on the oxygen atom lessens and is accompanied by a buildup of positive charge on the developing sp^2 hybridized orbital of the carbon atom. Due to the overlap between the incipient carbocationic center and the singly occupied p-orbital, charge transmission to the aromatic substituent is now possible in the transition state.

The other parameter obtained from treatment of the data with eq 5 is the acidity constant, K_a, for the protonated radical, Table 1. These values are not strongly affected by the nature of the substituent, presumably due to the absence of a direct resonance interaction between the aromatic ring and the protonated hydroxyl group. It would be useful to convert the pK_a values measured in HFIP to pK_a values in water. Previous work has shown that ammonium ions are less acidic by 4.5 pK_a units in HFIP than in aqueous solution.[52] Assuming a similar difference applies to the protonated β-OH radicals, the measured pK_a values near 1.5 in HFIP can be used to estimate acidity constants near p$K_a \approx -3$ for protonated radicals **2a−d** in aqueous solution, values which are similar to p$K_a \approx -2.5$ for simple protonated alcohols like methanol or ethanol in water. In addition, pK_a values for protonated alcohols in acetonitrile were found to be near 2.3,[53] which is quite close to the p$K_a = 2.6$ for protonated radical **2e** in the same solvent. Given these similarities, it is reasonable to conclude that the protonated radicals **2a−e** have acidities that differ little from those of protonated alcohols, and that the presence of the α-radical center has little influence on the acidity constant of the protonated OH group.

Mechanism of and Solvent Effect on Reaction of β-OH Radical 2e. In acidic acetonitrile, TFE, and TFE/acetonitrile mixtures, curvature in the relationship between the observed rate constant for β-heterolysis of radical **2e** and acid concentration was observed, leading to the values for k_{het} and K_a summarized in Table 1. An interesting feature of these data is that the rate constants, k_{het}, for elimination of water from the protonated radical **2e** increase only 10-fold upon going from acetonitrile to TFE. This behavior is quite different from the solvent effect on the rate constants for cleavage of β-substituted radicals with different leaving groups, namely the ionization reactions of bromide,[11] chloride,[11] and mesylate[12] from β-substituted 4-methoxyphenethyl radicals that increase about 2 orders of magnitude upon going from ca. 20% TFE in acetonitrile to neat TFE, Figure 6. There are noteworthy differences between

(50) Bansal, K. M.; Gratzel, M.; Henglein, A.; Janata, E. *J. Phys. Chem.* **1973**, *77*, 16−19.

(51) Hansch, C.; Leo, A.; Taft, R. W. *Chem. Rev.* **1991**, *91*, 165−195.

(52) Carre, B.; Devynck, J. *Anal. Chim. Acta* **1981**, *131*, 141−147.

(53) Kolthoff, I. M.; Chantooni, M. K., Jr. *J. Am. Chem. Soc* **1968**, *90*, 3320−3326.

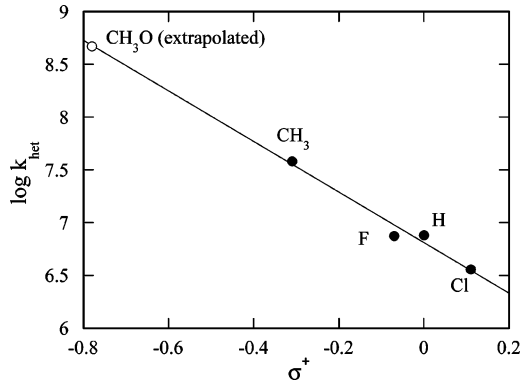

FIGURE 5. Correlation analysis of rate constant k_{het} in acidic HFIP as a function of σ^+ [51] for the elimination of water from β-OH radicals **2a**−**d**. The data point for radical **2e** was estimated by using the slope and $\sigma^+(CH_3O) = -0.78$.

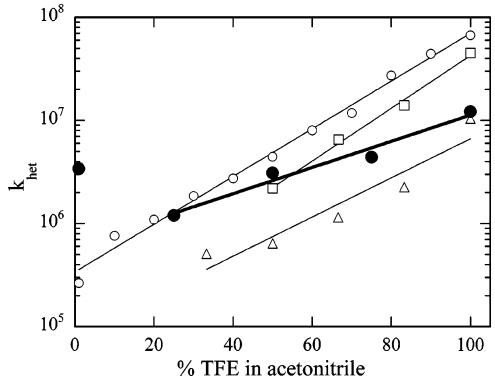

FIGURE 6. Rate constants for heterolysis of (●) water, (Δ) chloride, (□) bromide ,and (○) mesylate from β-substituted 4-methoxyphenethyl radicals as a function of TFE in acetonitrile.

the heterolysis reaction of radical **2e** and radicals with bromide, chloride, or mesylate as the leaving group. In particular, significant charge formation occurs in the transition states for the ionization of the latter three radicals, and these transition states are likely to be increasingly stabilized as the ionizing ability of the solvent increases. On the other hand, protonated radical **2e** is a distonic radical cation already carrying a full positive charge. Consequently, only charge redistribution and not charge buildup takes place as the reaction proceeds, and there is less favorable differential solvation of the transition state relative to the starting state as the polarity or ionizing ability of the solvent increases upon going to neat TFE.

A substantial decrease in pK_a values was observed upon going from neat AcN to neat TFE. This decrease in acidity is consistent with cationic acids like ammonium ions and protonated alcohols being more acidic in TFE[52] than AcN.[53] In addition, a p$K_a \approx$ 1.3 for protonated **2e** in HFIP can be estimated on the basis of the lack of a substituent effect on the acidities of protonated radicals **2a**−**d**. This estimated pK_a in HFIP is about 0.3 pK_a units larger than the pK_a of 1.0 for the same protonated radical in TFE, which is also consistent with the weaker acidity of ammonium ions in HFIP compared to TFE.[52]

In HFIP, no curvature was observed in the relationship between the observed rate constants for radical cation formation and acid concentration. It is possible that the lack of curvature was due to the required use of only low concentrations of perchloric acid (vide supra). If so, the slope of the plot in Figure 4b would represent the ratio $k_{het}/K_a = 7.8 \times 10^8$ M^{-1} s^{-1}. Assuming K_a for protonated **2e** in HFIP is near 1.3, then k_{het} for this protonated radical would be 4×10^7 s^{-1}. This rate constant is roughly the same as that for elimination of water from the 4-methyl derivative, **2d**, and about 10-fold smaller than a rate constant of ca. 5×10^8 s^{-1} that can be estimated from the Hammett relationship in Figure 5. Thus, it is likely that a different mechanism is responsible for the reaction of **2e** in HFIP. An alternative mechanism is one where, due to the presence of the electron-donating 4-methoxy group, loss of water becomes more rapid than protonation. This situation has been observed previously in the general acid-catalyzed reaction of α-methoxy ketyl radicals generated in aqueous solution.[25] Thus, for radical **2e** in HFIP, the measured rate constant of 7.8×10^8 M^{-1} s^{-1} most likely represents the rate constant for protonation, rather than being a combination of the β-heterolysis rate constant, k_{het}, and the acidity of the protonated radical, K_a.

In summary, the loss of OH from the photogenerated β-OH radicals was readily monitored due to the strong absorbance and relatively long lifetime of the initially produced styrene radical cations. The dependence of the rate constants for conversion of the β-OH radicals to the radical cations in various solvents indicates the reaction involves a rapid pre-equilibrium protonation of the β-OH group, followed by rate-limiting elimination of water. The one exception is the reaction of the 4-CH_3O-substituted radical in HFIP that appears to occur via a general acid-catalyzed mechanism.

Experimental Section

Materials. Spectroscopic grade acetonitrile, 1,1,1,3,3,3-hexafluoroisopropanol, and 2,2,2-trifluoroethanol were commercially available and used as received. The detailed preparation of precursors **1a**−**e** has been described previously.[12]

Laser Flash Photolysis. The nanosecond laser flash photolysis system at Dalhousie University is of standard design and has been previously described.[11] Samples for laser experiments were prepared in square 7×7 mm^2 laser cells manufactured from Suprasil quartz tubing. Each cell contained a 1 mL aliquot of solution and was capped with a rubber septum. Unless otherwise specified, samples were deaerated with ultrahigh purity (UHP) nitrogen or oxygen for 15 min prior to injecting the precursor compound previously dissolved in AcN. The injection volumes ranged from 4 to 10 μL and generated precursor concentrations between 10 and 30 mM within the laser cell. These were adjusted such that the maximum absorbance of the solution was in the range of 0.4−0.6 at the excitation wavelength of 266 nm (fourth harmonic from a Nd:YAG laser; ≤8 ns/pulse; ≤20 mJ/pulse). To prepare the acidic solutions, 1.0 M $HClO_4$ in the appropriate solvent (HFIP, TFE, AcN, or TFE/AcN mixture) was first prepared with standardized 70% perchloric acid. This 1.0 M $HClO_4$ stock solution was then diluted with the appropriate solvent to give the desired acid concentrations. All experiments were carried out at room temperature (22 ± 1 °C).

The thermal stability of the precursor compounds in acidic solutions was verified prior to experimentation. The precursor compound was injected into a solution of the strongest acid concentration studied and monitored every 5 min for a period of an hour by UV spectroscopy. Absorption changes were not observed under these experimental conditions.

Note Added after ASAP Publication. Errors were corrected in Table 1 and published on December 7, 2007.

Acknowledgment. The authors gratefully acknowledge the Natural Sciences and Engineering Research Council of Canada (NSERC) for financial support of this research. S.F.L. thanks NSERC and the Izaak Walton Killam Memorial Foundation for postgraduate scholarships.

JO701874F